6-2013

Gsx2 controls region-specific activation of neural stem cells and injury-induced neurogenesis in the adult subventricular zone

Alejandro Lopez-Juarez
The University of Texas Rio Grande Valley

Jennifer Howard

Kristy Ullom

Lindsey Howard

Andrew Grande

Recommended Citation

López-Juárez, A., Howard, J., Ullom, K., Howard, L., Grande, A., Pardo, A., Waclaw, R., Sun, Y. Y., Yang, D., Kuan, C. Y., Campbell, K., & Nakafuku, M. (2013). Gsx2 controls region-specific activation of neural stem cells and injury-induced neurogenesis in the adult subventricular zone. Genes & development, 27(11), 1272–1287. https://doi.org/10.1101/gad.217539.113

Gsx2 controls region-specific activation of neural stem cells and injury-induced neurogenesis in the adult subventricular zone

Alejandro López-Juárez,[1] Jennifer Howard,[1] Kristy Ullom,[1] Lindsey Howard,[1] Andrew Grande,[1,2,6] Andrea Pardo,[1,7] Ronald Waclaw,[1,3,4] Yu-Yo Sun,[1,8] Dianer Yang,[1,8] Chia-Yi Kuan,[1,4,8] Kenneth Campbell,[1,2,4,5] and Masato Nakafuku[1,2,4,9]

[1]Division of Developmental Biology, Cincinnati Children's Hospital Research Foundation, Cincinnati, Ohio 45229, USA; [2]Department of Neurosurgery, University of Cincinnati College of Medicine, Cincinnati, Ohio 45267, USA; [3]Division of Experimental Hematology and Cancer Biology, Cincinnati Children's Hospital Research Foundation, Cincinnati, Ohio 45229, USA; [4]Department of Pediatrics, University of Cincinnati College of Medicine, Cincinnati, Ohio 45267, USA; [5]Division of Neurosurgery, Cincinnati Children's Hospital Research Foundation, Cincinnati, Ohio 45229, USA

Neural stem cells (NSCs) reside in widespread regions along the lateral ventricle and generate diverse olfactory bulb (OB) interneuron subtypes in the adult mouse brain. Molecular mechanisms underlying their regional diversity, however, are not well understood. Here we show that the homeodomain transcription factor Gsx2 plays a crucial role in the region-specific control of adult NSCs in both persistent and injury-induced neurogenesis. In the intact brain, Gsx2 is expressed in a regionally restricted subset of NSCs and promotes the activation and lineage progression of stem cells, thereby controlling the production of selective OB neuron subtypes. Moreover, Gsx2 is ectopically induced in damaged brains outside its normal expression domains and is required for injury-induced neurogenesis in the subventricular zone (SVZ). These results demonstrate that mobilization of adult NSCs is controlled in a region-specific manner and that distinct mechanisms operate in continuous and injury-induced neurogenesis in the adult brain.

[*Keywords*: stem cell; adult neurogenesis; regional identity; injury; stroke]

Supplemental material is available for this article.

Received March 10, 2013; revised version accepted May 3, 2013.

Neural stem cells (NSCs) persist in adult animals across vertebrate species, and active production of new neurons (neurogenesis) by these endogenous stem cells appears to be widespread in the brain and spinal cord of fish and amphibian species (Kaslin et al. 2008). In mammals, however, continuous neurogenesis is restricted to a few specialized regions, including the subventricular zone (SVZ) lining the lateral ventricle (LV) and subgranular zone (SGZ) in the hippocampal dentate gyrus (DG) (Zhao et al. 2008). Recent studies have revealed common features of NSCs in these so-called neurogenic niches. In adults, NSCs remain quiescent or divide infrequently and persist throughout the life of animals, although their activity gradually declines over time (Morshead et al. 1994; Doetsch et al. 1999; Maslov et al. 2004; Shook et al. 2012). These quiescent and slowly cycling (activated) stem cells (hereafter called qNSCs and aNSCs, respectively) share some features with astroglia in adults and radial glia in embryos, such as the expression of glial fibrillary acidic protein (GFAP) and the glial high-affinity glutamate transporter GLAST (Pastrana et al. 2009; Beckervordersandforth et al. 2010). aNSCs divide slowly over time, but once they progress to transient amplifying progenitors (TAPs), the cells undergo several rounds of rapid cell divisions and subsequently differentiate into neuroblasts (NBs) or glial cells (Doetsch et al. 1999; Bonaguidi et al. 2011). These nascent NBs exit the stem cell niche and migrate to their destinations, such as the olfactory bulb (OB) and DG, and are subsequently integrated into the circuitry (Ming and Song 2005).

Recent studies have identified many common regulatory mechanisms by which the maintenance and lineage

Present addresses: [6]Department of Neurosurgery, University of Minnesota, Minneapolis, MN 55455, USA; [7]Department of Neurology, Loma Linda University School of Medicine, Loma Linda, CA 92354, USA; [8]Department of Neurology, Emory University, 505H Whitehead Research Building 615, Michael Street, Atlanta, GA 30322
[9]Corresponding author
E-mail masato.nakafuku@cchmc.org
Article published online ahead of print. Article and publication date are online at http://www.genesdev.org/cgi/doi/10.1101/gad.217539.113.

progression of stem cells are controlled in the adult SVZ and DG (Ninkovic and Götz 2007). Not surprisingly, many of these mechanisms are also common between stem/progenitor cells in embryos and adults. However, one notable difference is that most, if not all, stem/progenitor cells in embryos undergo rapid cell divisions, whereas adult NSCs remain mostly quiescent or divide infrequently (Morshead et al. 1994; Maslov et al. 2004; Bonaguidi et al. 2011). Thus, the long-term maintenance of NSCs and their lineage progression to TAPs, the first step in mobilization of NSCs toward neurogenesis, is not only unique but also crucial for persistent adult neurogenesis. Such regulatory steps appear common in the long-lasting stem cell systems of many adult organs and tissues, but the underlying mechanisms are not well understood (Simons and Clevers 2011).

Beside these common features, there are some important differences between stem cells in the SVZ and DG. One notable distinction is that NSCs in the DG generate only a single neuronal subtype, DG granule cells, whereas those in the SVZ produce multiple distinct neuronal subtypes that populate different laminae of the OB and exert distinct physiological functions (Lledo et al. 2008). Moreover, a recent study has reported that the overall ratio of the production of these diverse OB neuron subtypes is maintained over an extended period in adults (Shook et al. 2012). As a mechanism underlying such neuronal diversity, recent studies have provided evidence that NSCs residing in distinct subregions of the SVZ are committed to generating different neuronal subtypes (Merkle et al. 2007). In fact, NSCs distribute widely along the dorsoventral (DV) and anterior–posterior (AP) axes of the LV (Mirzadeh et al. 2008). Recent studies have also shown that the rostral migratory stream (RMS)—a specialized migratory path for NBs from the SVZ to the OB—and the OB itself contain NSCs (Gritti et al. 2002; Giachino and Taylor 2009). Details of such regional specificity of NSCs, however, are largely unknown.

In this study, we show that the homeodomain transcription factor Gsx2 plays an important role in such region-specific control of adult NSCs. Our conditional loss-of-function (LOF) and gain-of-function (GOF) analyses in vivo demonstrate that Gsx2 promotes the activation and subsequent lineage progression in a discrete subset of NSCs in the adult SVZ, thereby controlling the production of specific OB neuron subtypes. Moreover, we found that hypoxia–ischemia (H/I) and neurotoxic injury induce Gsx2 in widespread regions of the stem cell niche and that such ectopic Gsx2 plays a crucial role in injury-induced neurogenesis. Thus, Gsx2 is a crucial region-specific regulator of adult NSCs in both continuous neurogenesis and injury-induced regenerative responses.

Results

Regionally restricted expression of Gsx2 in the adult SVZ

To facilitate expression analysis of Gsx2 in the adult brain, we used a Gsx2-specific antibody (Toresson et al. 2000) as well as $Gsx2^{GFP\text{-}KI/+}$ mice in which the cDNA for green fluorescent protein (GFP) is knocked into the *Gsx2* locus, and thus GFP recapitulates the expression of endogenous Gsx2 (Wang et al. 2009). In coronal sections of the adult brain, where the LV is maximally extended along the DV axis, a cluster of $Gsx2^+$/Gsx2-GFP^+ cells were found in the dorsolateral (dl) region of the SVZ, forming a narrow arcuate band flanked by the striatum ventrolaterally and the corpus callosum (CC) and LV dorsally and medially, respectively (Fig. 1A–C‴). Although a few $Gsx2^+$ cells were also detected along the lateral (l) wall of the LV, they were rare in the dorsal roof (dr), medial (m), and ventral (v) regions (Fig. 1D–D″). Thus, the vast majority of $Gsx2^+$ cells (93.4% ± 16.7%, $n = 4$ animals) are confined to the dlSVZ (Supplemental Fig. 1F). This region-restricted expression of Gsx2 is in sharp contrast to the much broader expression patterns of Ascl1, Dlx2, and Ki67 that represent active neurogenesis all along the LV (Supplemental Fig. 1A–A″,F). Thus, among broad neurogenic niches, Gsx2 expression is confined to one of the predominantly active regions, the dlSVZ. We detected similar numbers of $Gsx2^+$ cells in the same region of young and mature adult animals (2 and 10 mo old, respectively) (Fig. 3C, below; data not shown).

We further characterized the specificity of Gsx2 expression along the AP axis of the brain. The dorsally restricted expression of Gsx2 is maintained in the posterior SVZ, adjacent to the striatum laterally and the hippocampal fimbria medially (Fig. 1G,H). Notably, no $Gsx2^+$ cells were detected in the SGZ of the DG, another known stem cell niche (data not shown). However, a small number of $Gsx2^+$ cells were detected in the periventricular region overlaying the hippocampus where NSCs contribute to injury-induced neurogenesis (Fig. 1H; Nakatomi et al. 2002). Along the anteriormost part of the LV, $Gsx2^+$ cells were found all along the SVZ (Fig. 1F). The lack of the DV selectivity in this region is probably because the dorsal domain is disproportionally represented relative to its ventral counterpart in the coronal plane, while the LV gradually converges anteriorly into the ventrally located RMS (Fig. 1A). More anteriorly, the anterior RMS contains fewer $Gsx2^+$ than its posterior half, and no $Gsx2^+$ cells were found in the OB (Fig. 1E–E″; data not shown). Thus, $Gsx2^+$ cells are widespread along the AP axis yet confined to a restricted subset of cells along the DV axis.

Previous studies have shown the dorsally restricted expression of the homeodomain factor Pax6 and the zinc finger factor Sp8 in the SVZ, but which cell types express these transcription factors remains uncharacterized (Hack et al. 2005; Kohwi et al. 2005; Waclaw et al. 2006). We found that ~44% and 37% of Gsx2-GFP^+ cells in the dlSVZ express Pax6 and Sp8, respectively, but few cells coexpress all three (Fig. 1I–J‴). Moreover, many more $Pax6^+$ and $Sp8^+$ cells were found than Gsx2-GFP^+ cells, and these $Gsx2^-$/$Pax6^+$ and $Gsx2^-$/$Sp8^+$ cells were mutually exclusive populations that corresponded to $Dlx2^+$ NBs (Fig. 1I,K; Supplemental Fig. 1G). An exception was $Pax6^+$ cells in the dorsal roof region (drSVZ or pallial SVZ), where few $Gsx2^+$ cells were found (Figs. 1I, 3N).

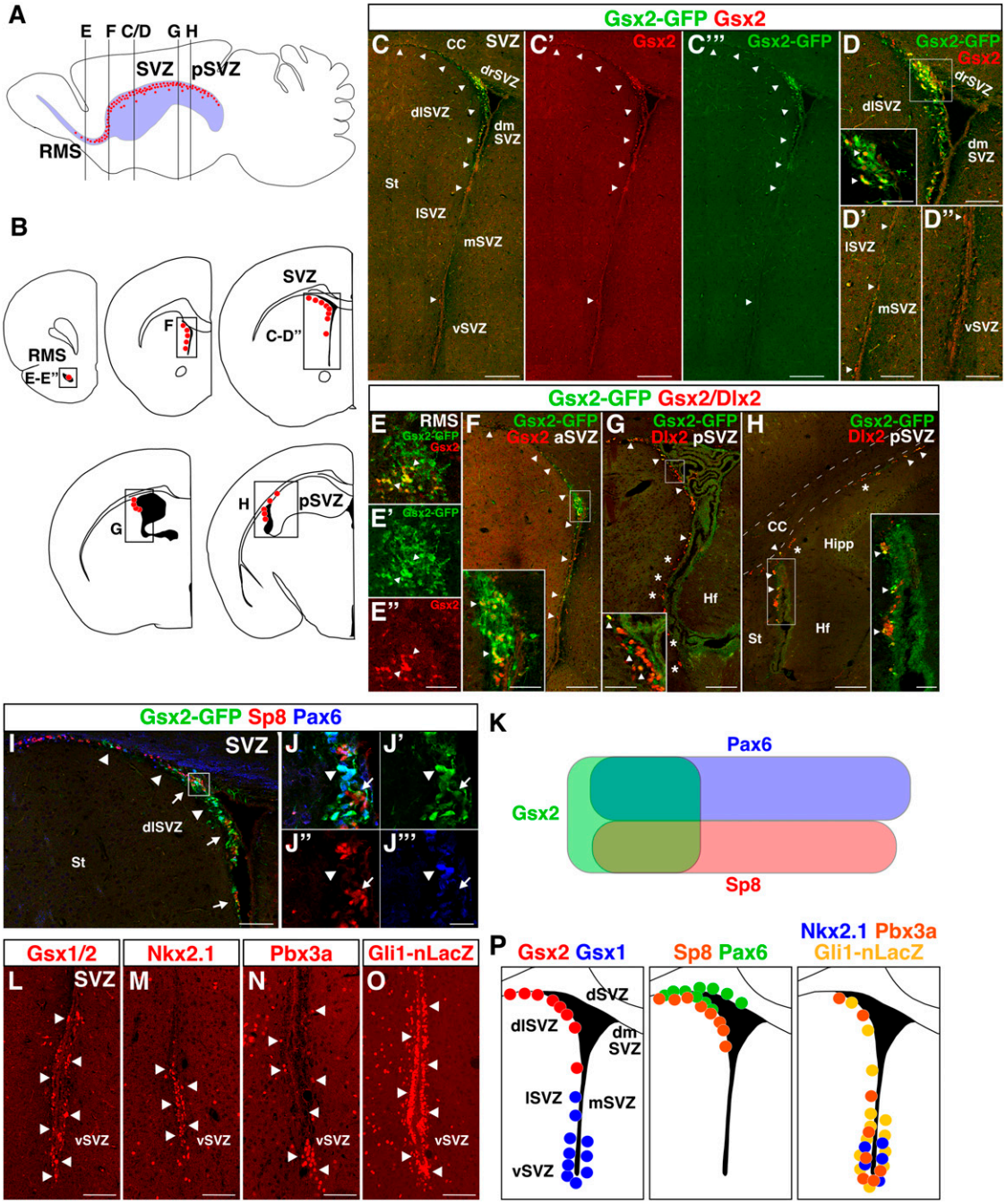

Figure 1. Regionally restricted expression of Gsx2 in the adult neurogenic niche. (*A*,*B*) Schematic representations of the OB–RMS–SVZ stem cell niches. Vertical lines in *A* and boxed areas in *B* indicate the approximate locations of the areas shown in *C*–*H*. Red dots indicate the location of Gsx2$^+$ cells. (*C*–*D*″) Dorsally restricted expression of Gsx2 and Gsx2-GFP (arrowheads) in the SVZ (a higher-magnification view is in the *inset* in *D*). Few Gsx2$^+$ cells are found in l/mSVZ (*D*′) or vSVZ (*D*″). (*E*–*H*) Expression of Gsx2 in the RMS (*E*–*E*″) and the anterior (*F*) as well as posterior (*G*,*H*) SVZ (higher-magnification views are in the *insets*). Asterisks in *G* and *H* indicate the distribution of Dlx2$^+$ cells beyond the ventral limit of Gsx2$^+$ cells. (*I*–*K*) Overlapping expression of Gsx2-GFP with Pax6 (arrowheads) and Sp8 (arrows) in *Gsx2*$^{GFP\text{-}KI/+}$ mice. (*L*–*O*) Expression of Gsx1/2 (pan-Gsx)$^+$ (*L*), Nkx2.1 (*M*), Pbx3a (*O*), and Gli1-nLacZ (*N*) in the vSVZ. (*P*) Schematic representations of the expression patterns of Gsx1 and Gsx2 (*left*), Pax6 and Sp8 (*middle*), and Nkx2.1, Pbx3a, and Gli1-nLacZ (*right*) along the DV axis of the SVZ. Bars: *C*–*C*‴,*F*–*H*, 200 μm; *D*–*D*″,*I*,*L*–*O*, 100 μm; *E*–*E*‴, *insets* in *D*,*F*–*H*, 50 μm; *J*-*J*‴, 10 μm.

More ventrally, staining with an antibody that detects both Gsx2 and its close homolog, Gsx1 (i.e., pan-Gsx) (Kriks et al. 2005), detected cells not only in the dlSVZ, but also in other regions of the SVZ, except for the dorsal roof (Fig. 1L; Supplemental Fig. 1C). Further analysis using *Gsx1-EGFP* mice from GENSAT (http://www.gensat.org) (Pei et al. 2011) demonstrated that Gsx1-GFP and Gsx2 show clear complementary patterns along the DV axis

(Supplemental Fig. 1B). Moreover, as described below, conditional inactivation of Gsx2 eliminated cells detected by the pan-Gsx antibody in the dlSVZ but not in the lSVZ or vSVZ (Supplemental Fig. 3J–K′). Thus, Gsx1 and Gsx2 are likely to be expressed in distinct sets of cells. Two other homeodomain factors, Nkx2.1 and Pbx3a, also showed expression patterns complementary to Gsx2 (Fig. 1M,N). Finally, in *Gli1-nLacZ* mice, in which the nuclear targeted LacZ transgene is knocked into the Shh-responsive *Gli1* gene (Bai et al. 2002), a large cluster of Gli1-nLacZ$^+$ cells surrounded the vSVZ, and fewer immunoreactive cells resided dorsally (Fig. 1O, Supplemental Fig. 1D–E″; Balordi and Fishell 2007). We found no overlap between Gli1-nLacZ and Gsx2 in the dlSVZ or lSVZ. Together, these results demonstrate that Gsx2 is expressed in a regionally restricted subset of cells in the adult SVZ and that such Gsx2$^+$ cells partially overlap with Pax6$^+$ and Sp8$^+$ cells dorsally but are segregated from Gsx1$^+$, Pbx3a$^+$, Nkx2.1$^+$, and Gli1-nLacZ$^+$ cells ventrally (summarized in Fig. 1P).

Gsx2 is expressed in aNSCs and TAPs

We next examined which cell types express Gsx2 in the adult neurogenic niche. Gsx2 expression was found only in a small fraction of total cells in these regions (9.2% and 5.9% of total DAPI$^+$ cells in the dlSVZ and RMS, respectively) (Supplemental Fig. 1F). However, the majority (78%) of Gsx2$^+$ cells coexpressed the basic helix–loop–helix (bHLH) transcription factor Ascl1, a well-defined marker for aNSCs and TAPs (Pastrana et al. 2009; Kim et al. 2011), and conversely, about one-third (34%) of Ascl1$^+$ cells coexpressed Gsx2 (Fig. 2D; Supplemental Fig. 2H). Coexpression of GFAP and epidermal growth factor receptor (EGFR) was also found in 16% and 91%, respectively, of Gsx2$^+$ cells (Fig. 2A,F; Supplemental Fig. 2H). In contrast, we detected no overlap between Gsx2$^+$ cells and doublecortin$^+$ (Dcx$^+$) NBs (Fig. 2B; Supplemental Fig. 2H). These results indicate that Gsx2 is predominantly expressed in NSCs and/or TAPs but not in NBs. In fact, approximately one-fourth of neurospheres established from the entire SVZ of wild-type mice contained Gsx2$^+$ cells (24.7% ± 7.6%, n = 3 independent culture experiments, total 328 neurospheres examined). Neurospheres from *Gsx2$^{GFP\text{-}KI/+}$* mice also contained GFP$^+$/Gsx2$^+$ cells, and such cells also expressed Sox2 (Fig. 2I–J″). Moreover, many GFP$^+$ cells in neurospheres derived from *Pax6-GFP* mice (Gong et al. 2003) expressed Gsx2, recapitulating the coexpression of Pax6 and Gsx2 in vivo (Fig. 2K–K″). However, a significant fraction (16%) of Gsx2$^+$ cells were Ki67$^-$ in vivo, suggesting that Gsx2 is also expressed in quiescent and/or slowly cycling cells (Fig. 2C; Supplemental Fig. 2H).

To further examine the mode of proliferation of Gsx2$^+$ cells, we used two paradigms of 5-bromo-2′-deoxyuridine (BrdU) labeling. TAPs and NBs are rapidly dividing cell types in the SVZ (Ponti et al. 2013). Therefore, the majority of cells labeled with BrdU shortly (2 h) after its administration are considered as TAPs and NBs. We found that >50% of short-term BrdU-labeled cells in the dlSVZ and RMS are Gsx2$^+$, consistent with the idea that Gsx2 is expressed in TAPs (Fig. 2G–G‴; Supplemental Fig. 2H). On the other hand, when cells are exposed to BrdU for an extended period and subsequently left unlabeled long enough (3 and 4 wk, respectively), NSCs, but not TAPs or NBs, are thought to be the predominant cell type among BrdU label-retaining cells (LRCs) (Maslov et al. 2004). Given that the transition between qNSCs and aNSCs could be reversible (Maslov et al. 2004; Basak et al. 2012), some of these BrdU-LRCs may also include qNSCs at the time of analysis. We found that Gsx2 expression was detected in a significant fraction of BrdU-LRCs (50% and 27% in the dlSVZ and RMS, respectively), indicating that Gsx2 is expressed in aNSCs and/or qNSCs (Fig. 2H–H″; Supplemental Fig. 2H). In line with this idea, ~14% of Gsx2$^+$ cells expressed both GFAP and EGFR (GFAP$^+$/EGFR$^+$), and a smaller fraction (9%) were GFAP$^+$/EGFR$^-$, consistent with the marker expression in aNSCs and qNSCs, respectively (Fig. 2F–F3; Supplemental Fig. 2I; Pastrana et al. 2009). Similar expression patterns were found in the RMS (Supplemental Fig. 2A–H). These data demonstrate that Gsx2 is one of the earliest genes expressed during the lineage progression of NSCs, coinciding with or slightly preceding Ascl1 and EGFR, two known markers for aNSCs and TAPs. However, a large fraction of Ascl1$^+$ and Dlx2$^+$ cells are negative for Gsx2 (66% and 78%, respectively), indicating that Gsx2 expression is transient and down-regulated when cells further proceed to Dlx2$^+$ TAPs and NBs (summarized in Fig. 2L). It is also possible, however, that some TAPs derive from Gsx2-nonexpressing cells.

Gsx2 is a region-specific regulator of adult neurogenesis

Mice homozygous for a null allele of *Gsx2* die at birth, precluding functional analysis of Gsx2 in adults (Szucsik et al. 1997). Therefore, we used the CreER-loxP system for its conditional inactivation. We generated mice homozygous for a floxed allele of *Gsx2* (*Gsx2^{flox}*) (Waclaw et al. 2009) and heterozygous for a *GLAST-CreER* knock-in allele (Mori et al. 2006). The latter contains a CreER transgene expressed from the locus of the glutamate transporter gene *GLAST* so that CreER is expressed in GFAP$^+$/GLAST$^+$ adult stem cells. The mice also carried the *CAG-CAT (CC)-EGFP* Cre reporter allele that allowed us to track the fate of recombined cells as GFP$^+$ cells (Nakamura et al. 2006). *GLAST-CreER;CC-EGFP* mice carrying *Gsx2$^{+/+}$* and *Gsx2$^{flox/+}$* showed no noticeable differences compared with the wild-type mice and therefore were used as control for *Gsx2* conditional knockout (cKO) (*Gsx2$^{flox/flox}$;GLAST-CreER;CC-EGFP*) mice. The CreER activator tamoxifen (Tx) was administered to these animals at the age of 8–12 wk and subsequently analyzed 9 and 56 d after the first Tx treatment (hereafter D9 and D56, respectively). A whole-mount view of the SVZ demonstrated widespread recombination in the SVZ of Tx-treated animals (Supplemental Fig. 3A). Moreover, the distribution pattern of GFP$^+$ cells along the DV axis of the LV was similar to that of Dlx2$^+$ and Ki67$^+$

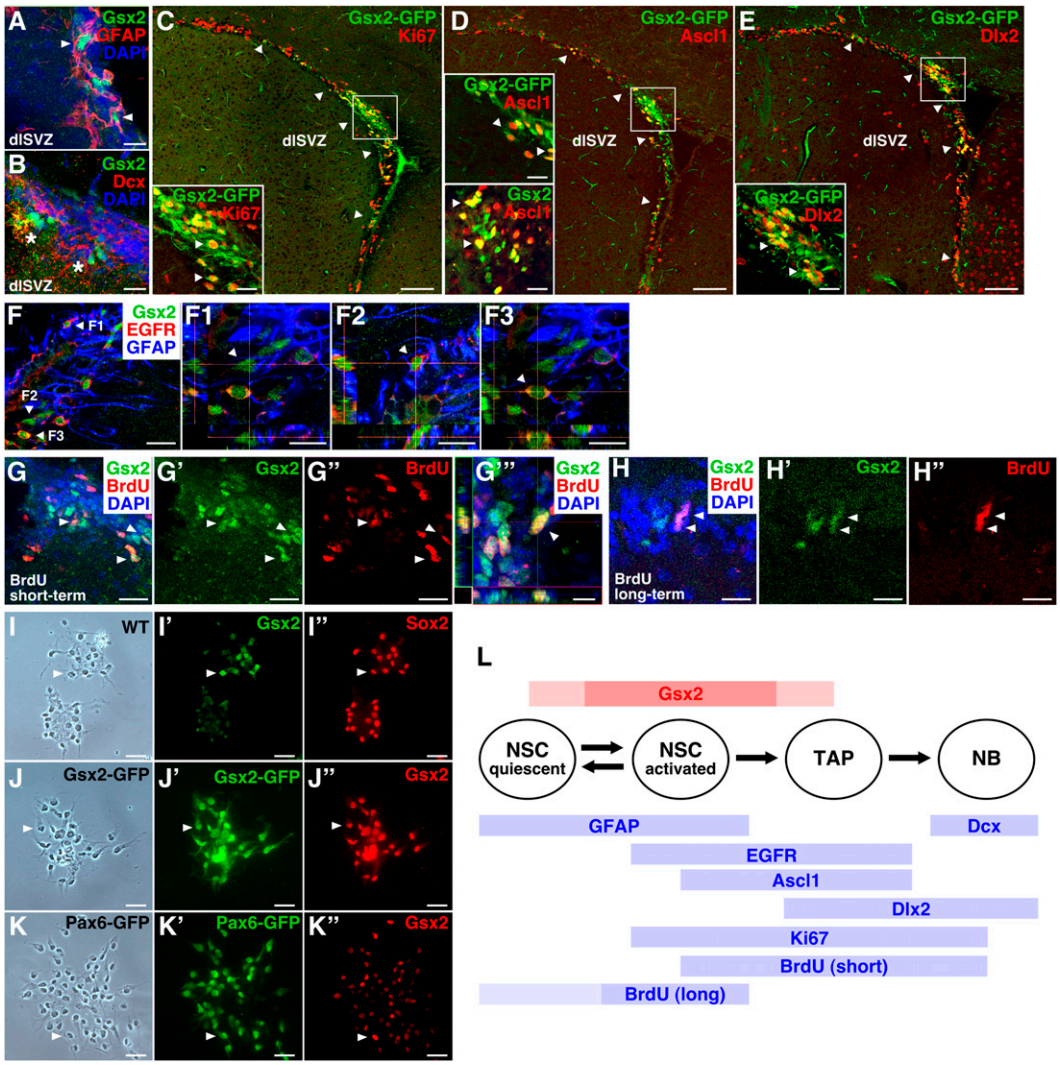

Figure 2. Expression of Gsx2 in NSCs and TAPs. (*A–H″*) Representative images of the dlSVZ costained for Gsx2 and a series of cell type-specific markers. *C–E* are imaged from *Gsx2*$^{GFP\text{-}KI/+}$ mice. Gsx2 and Gsx2-GFP are expressed in a subset of GFAP$^+$ (*A*), Ki67$^+$ (*C*), Aslc1$^+$ (*D*), and Dlx2$^+$ (*E*) NSCs and TAPs but not in Dcx$^+$ NBs (*B*) (higher-magnification views are in the *insets* in *C–E*). (*F–F3*) Confocal images of Gsx2$^+$ cells corresponding to a GFAP$^+$/EGFP$^-$ qNSC (*F1*), GFAP$^+$/EGFR$^+$ aNSC (*F2*), and GFAP$^-$/EGFR$^+$ TAP (F3). (*G–H′*) Gsx2$^+$ cells colabeled with BrdU (arrowheads) after short-term (*G–G‴*) and long-term (*H–H″*) labeling. (*I–K″*) Gsx2$^+$ cells in neurospheres derived from the adult SVZ. Coexpression of Gsx2 and Sox2 (*I–I″*), Gsx2-GFP and Sox2 (*J–J″*), and Pax6-GFP and Gsx2 (*K–K″*) (arrowheads) are detected in neurospheres. (*L*) Schematic representations of the expression of Gsx2 and other markers in the stem cell lineage. Bars: *C–E*, 100 μm; *A*,*B*,*F*,*G–G″*,*H–H″*,*I–K″*, insets in *C–E*, 20 μm; *F1–F3*, 10 μm; *G‴*, 5 μm.

cells, demonstrating regionally unbiased recombination (Supplemental Fig. 3B–G). Although no significant differences were found at D9, the number of Gsx2$^+$ cells in the dlSVZ markedly decreased at D56 in cKO mice compared with control (85% and 57% reductions in the anterior and posterior SVZs, respectively) (Fig. 3A–C). A smaller but significant decrease (43%) was also observed in the RMS (Fig. 3D,E). We assume that this delayed reduction of Gsx2$^+$ cells is because of the extremely slow turnover of GLAST$^+$ adult NSCs (Doetsch et al. 1999).

Nevertheless, once Gsx2 inactivation reached a significant level, it resulted in a severe reduction of neurogenesis in the dlSVZ. Ascl1$^+$, Ki67$^+$, and Dlx2$^+$ cells were substantially reduced in *Gsx2* cKO mice, demonstrating that the production of TAPs and NBs are attenuated (Fig. 3F–I). Importantly, such changes selectively occurred in the dlSVZ but not in other SVZ subregions, indicating that Gsx2 is a region-specific regulator of neurogenesis (Fig. 3J). Smaller yet significant reductions of TAPs and NBs were also detected in the RMS (Supplemental Fig. 3H–I′). The smaller impact of Gsx2 inactivation in the RMS is probably because Gsx2 is inactivated only partially in the RMS, and, moreover, NBs produced in all SVZ subregions converge in this region en route to the OB. In contrast, control and cKO mice showed no significant difference in the number of Olig2$^+$ cells in the dlSVZ or the percentage of Olig2$^+$ cells among GFP$^+$ progeny in

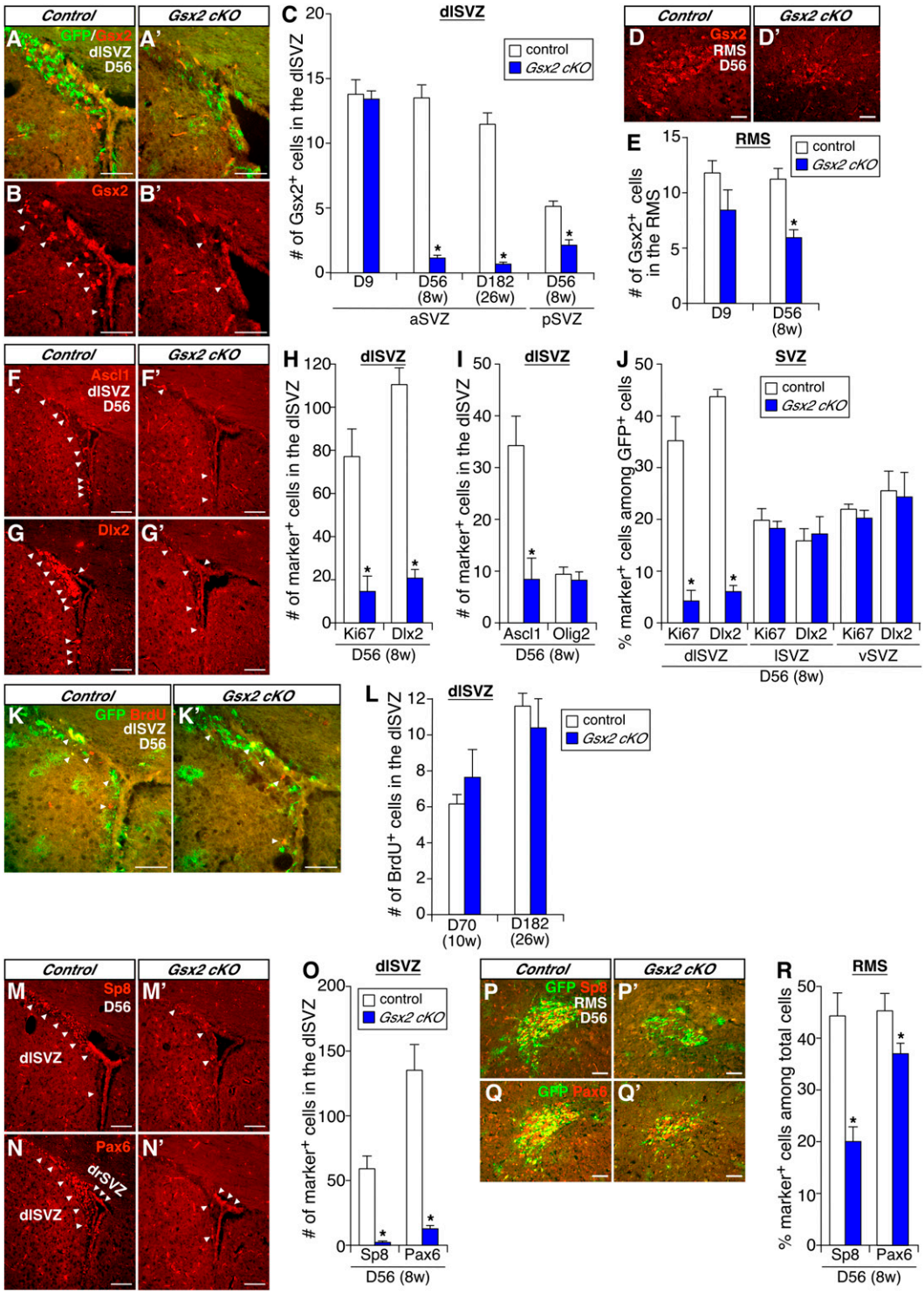

Figure 3. Conditional inactivation of Gsx2 leads to region-specific attenuation of neurogenesis. (*A–E*) Time-dependent loss of Gsx2$^+$ cells in the dlSVZ (*A–C*) and RMS (*D,E*) in *Gsx2* cKO mice. The number of Gsx2$^+$ cells in the anterior (a) and posterior (p) parts of the SVZ (*C*) and RMS (*E*) is compared between *Gsx2* cKO and control mice at D9, D56, and D182. (*F–L*) Region-specific attenuation of neurogenesis following inactivation of Gsx2. Ki67$^+$, Dlx2$^+$, and Ascl1$^+$ TAPs and NBs markedly decrease in the dlSVZ (*F–J*) but not in the lSVZ or vSVZ (*J*) of *Gsx2* cKO mice at D56. Olig2$^+$ cells (*I*) and BrdU-LRCs (*K–L*) remain unchanged. To detect LRCs, animals were treated with BrdU for 3 wk and subsequently left untreated for 4 wk before analysis. (*M–R*) Decrease of Sp8$^+$ and Pax6$^+$ cells in the dlSVZ (*M–O*) and RMS (*P–R*) in *Gsx2* cKO mice. Note that Pax6$^+$ cells remain in the drSVZ in the mutant. Data are expressed as mean ± SEM of three animals. (*) $P < 0.05$ compared with control animals. Bars: *A–B′*,*F–G′*,*K,K′*,*M–N′*, 100 μm; *D,D′*,*P–Q′*, 20 μm.

the OB, suggesting that gliogenesis is not affected by *Gsx2* inactivation (Fig. 3I).

We next asked at which step neurogenesis is blocked by Gsx2 inactivation. We observed a substantial decrease of both Ki67$^+$ cells and Ascl1$^+$ cells, suggesting that the production of TAPs is blocked in the mutant (Fig. 3H,I). However, the density of BrdU-LRCs in the dlSVZ was indistinguishable between control and cKO mice both 10 and 26 wk after Tx treatment (Fig. 3K–L). We did not detect significant differences in the percentages of GFAP$^+$/EGFR$^-$ qNSCs and GFAP$^+$/EGFR$^+$ aNSCs among GFP$^+$ cells between control and *Gsx2* cKO mice at D56 either (data not shown). These results support the idea that the NSC pool (qNSCs and aNSCs) is preserved in the mutant dlSVZ. Nevertheless, we did not detect any significant recovery of Gsx2$^+$ cells or the overall neurogenic activity 26 wk after Gsx2 inactivation (Fig. 3C). Thus, unlike in other organs or tissues, where expansion of neighboring or remaining stem cells occurs following a focal loss of stem cells (Simons and Clevers 2011), it appears that few remaining Gsx2$^+$ or Gsx2-nonexpressing NSCs undergo compensatory proliferation and recover the stem cell activity in the defective niche as previously observed for Shh signaling-deficient NSCs (Balordi and Fishell 2007). Together, these results demonstrate that Gsx2 plays an essential role in the lineage progression from aNSCs to TAPs in a subset of NSCs (see Fig. 5R, below).

We next examined whether the regional identity of NSCs is compromised in *Gsx2* cKO mice. We found a marked reduction of Sp8$^+$ and Pax6$^+$ cells in the dlSVZ of *Gsx2* cKO mice, although Pax6$^+$ cells in the dorsal roof region remained unaffected (Fig. 3M–O). We also detected a large reduction of Sp8$^+$ cells (45% of control) in the RMS, whereas Pax6$^+$ cells were mostly spared (83% of control) (Fig. 3P–R). Thus, the generation of Sp8$^+$ NBs appears to strongly depend on Gsx2 in both the SVZ and RMS, but Pax6$^+$ cells depend on Gsx2 only in the dlSVZ. Moreover, cells detected with the pan-Gsx antibody diminished in the dlSVZ but remained unchanged in other regions in the mutant, indicating no compensatory dorsal expansion of ventrally located Gsx1$^+$ cells (Supplemental Fig. 3J–K′), unlike in *Gsx2* mutant embryos (Toresson and Campbell 2001; Yun et al. 2003). The ventrally restricted expression of Nkx2.1 was also indistinguishable between *Gsx2* cKO and control mice (Supplemental Fig. 3L,L′). These results support the idea that inactivation of Gsx2 does not alter the regional identity of NSCs in the dlSVZ or lead to compensatory expansion of adjacent SVZ subdomains.

Gsx2 is required for production of selective subsets of OB neurons

We next examined the impact of Gsx2 inactivation on the specification of OB neuron subtypes. In both *Gsx2* cKO and control mice, the progeny of recombined NSCs are genetically labeled as GFP$^+$ cells so that the fate of OB neurons that are generated after Tx treatment can be tracked. Therefore, neuronal subtypes that have smaller representations among the total GFP$^+$ neurons in the *Gsx2* cKO OB compared with the control should be considered Gsx2-dependent.

First, we examined the laminar distribution of GFP-labeled new neurons in the OB at D56. In both control and cKO mice, GFP$^+$ cells were found in multiple layers, including the glomerular layer (GL), the external and internal plexiform layers (herein collectively called the intermediate layer [IL]), and the granule cell layer (GCL) (Fig. 4A). Although resident GLAST$^+$ astrocytes were also labeled as GFP$^+$ cells in these mice, such glial cells were easily distinguishable from GFP$^+$ neurons by their morphology and the lack of coexpression of Dlx2, a common marker for OB interneurons (Fig. 4B). In control mice, ~70% of GFP$^+$ neurons were found in the GCL, and a disproportionally larger fraction of them (50%) resided in its deeper one-third (dGCL), consistent with the distribution pattern of adult-born neurons (Fig. 4K; Lemasson et al. 2005). We detected no noticeable differences in the laminar distribution patterns between cKO and control mice. However, a significantly smaller fraction of GFP$^+$ GCL neurons expressed Mef2c (Lyons et al. 1995) in the cKO mice, and such a reduction was more pronounced in the dGCL (Fig. 4C,L). These results demonstrate that Gsx2 is required for the proper production of a selective subset of Mef2c$^+$ GCL neurons.

We next examined the GL where a greater variety of neuronal subtypes can be identified with a set of markers (Fig. 4D–H). Previous studies have shown that cells expressing calretinin (CR), neurocalcin (NC), calbindin (CB), tyrosine hydroxylase (TH), and parvalbumin (PV) represent discrete interneuron populations, except for a partial overlap between CR$^+$ and NC$^+$ cells (Briñón et al. 1999; Parrish-Aungst et al. 2007). Among total GFP-labeled GL neurons, a much smaller percentage of GFP$^+$ neurons expressed CR, NC, and CB in *Gsx2* cKO mice than in the control, whereas the proportions of TH$^+$ and PV$^+$ neurons remained unchanged (Fig. 4M). Moreover, Sp8$^+$ cells, which overlap with CR$^+$ and NC$^+$ neurons in the GL (Waclaw et al. 2006; data not shown), were much less represented in GFP$^+$ neurons, whereas Pax6$^+$ neurons were unaffected in cKO mice (Fig. 4I,J,M). As a result, a larger fraction of GFP-labeled adult-born neurons remained negative for all of these markers, raising the possibility that many GL neurons that normally differentiate into CR$^+$, CB$^+$, and NC$^+$ neurons either fail to differentiate or transform into currently unidentifiable neuronal subtypes. Tbr1$^+$ and Tbr2$^+$ glutamatergic interneurons (Brill et al. 2009) were barely (<0.1%) labeled with GFP in control mice and were not apparently affected in *Gsx2* cKO mice (data not shown).

Constitutive Gsx2 expression expands aNSCs and blocks neurogenesis

The aforementioned results have demonstrated that Gsx2 is required for neurogenesis in a regionally restricted subset of NSCs. We next asked whether it is sufficient to promote neurogenesis. To achieve temporally controlled overexpression, we used a combination of

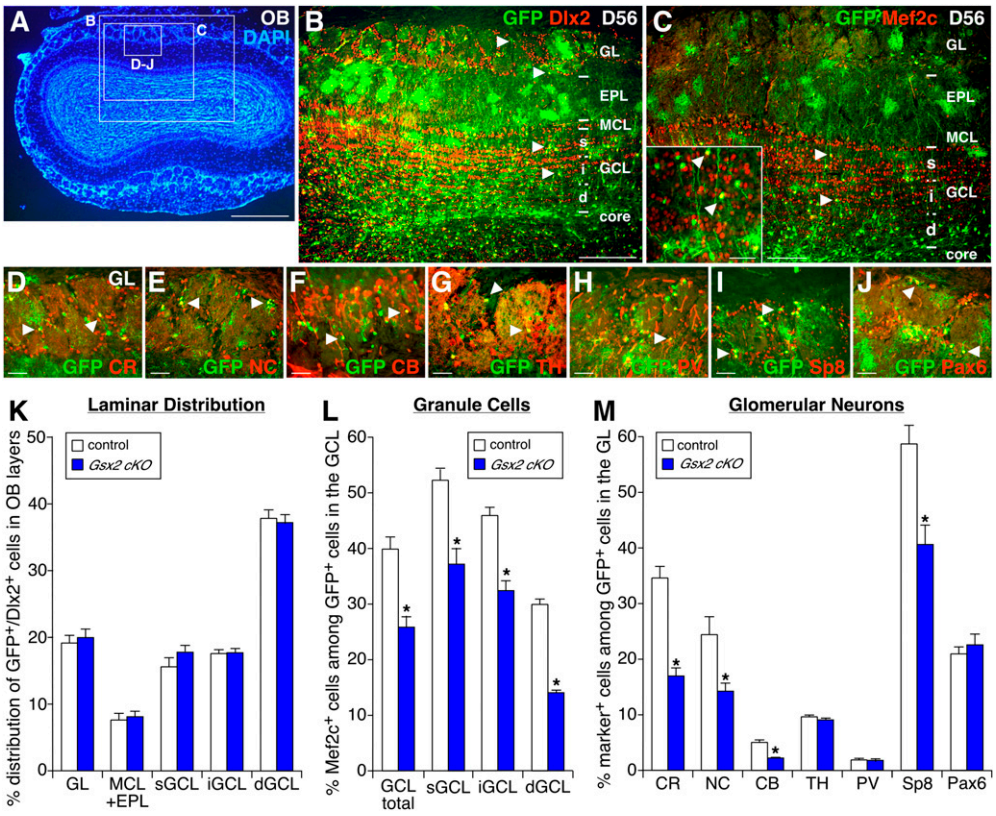

Figure 4. Attenuated production of selective subsets of OB interneurons in *Gsx2* cKO mice. (*A–J*) GFP-labeled OB neurons (arrowheads) in control mice at D56. (*A,B*) DAPI and GFP/Dlx2 costaining. Boxes in *A* indicate the locations of the areas shown in *B–J*. (*C*) GFP/Mef2c costaining in the GCL. (*D–J*) Overlap between GFP and various interneurons markers in the GL. (*K*) Laminar distribution pattern of GFP$^+$/Dlx2$^+$ fate-mapped neurons at D56. (*L*) The percentage of GFP-labeled neurons expressing Mef2c in the superficial (s), intermediate (i), and deep (d) layers as well as the whole GCL at D56. (*M*) The percentage of GFP-labeled neurons expressing various GL interneuron markers at D56. Data are expressed as mean ± SEM of four animals. (*) $P < 0.05$ compared with control animals. Bars: *A*, 500 μm; *B*, 200 μm; *C*, 100 μm; *D–J*, *inset* in *C*, 50 μm.

CreER-LoxP and *tetO-tTA* transgenic systems by generating *TetO-Gsx2-IRES-EGFP;GLAST-CreER; ROSA-LNL-tTA* mice (hereafter called *Gsx2 GOF* mice) and those carrying *TetO-IRES-EGFP* (control mice). In these mice, Tx induces the expression of the *TetO* promoter transactivator (tTA) in GLAST$^+$ SVZ stem cells by removing a stop cassette from *tTA* transgene knocked into the *ROSA26* locus (*ROSA-LNL-tTA*) (Wang et al. 2008). This tTA subsequently activates the *TetO* promoter-driven expression of Gsx2 and GFP in *Gsx2 GOF* mice and GFP alone in control mice (Waclaw et al. 2009). Thus, once induced by Tx, Gsx2 and GFP are constitutively expressed in NSCs and their progeny. Moreover, the activation of the TetO transgenes can be subsequently shut off by administering doxycycline (Dox), a suppressor of tTA, to the animals.

As shown in Figure 5, A–C, Tx-treated *Gsx2 GOF* mice robustly overexpressed Gsx2 in the SVZ. We detected more Gsx2$^+$ cells and a higher level of Gsx2 protein expression in each cell in its normal expression domain as well as in ectopic locations all around the LV. In control animals, however, the dlSVZ-restricted expression of Gsx2 remains unchanged (Supplemental Fig. 4A,A′), and many GFP-labeled, Dlx2$^+$ neurons reached the OB by D63 (Fig. 5L). Contrary to our expectation, most GFP$^+$ cells in the OB of *Gsx2 GOF* mice were astrocytes, and few GFP$^+$/Dlx2$^+$ new neurons were detected (Fig. 5M,Q). Few activated caspase-3$^+$ cells were detected anywhere along the OB–RMS–SVZ axis, and no ectopic GFP-labeled neurons were found outside these neurogenic regions, indicating that aberrant cell death or ectopic migration does not account for the absence of new GFP$^+$ neurons in *Gsx2 GOF* mice (data not shown).

We then examined the impact of Gsx2 overexpression on NSCs. In control animals, the production of new neurons by recombined NSCs reached a steady-state level by D63 so that GFP labeling covers the entire lineage from GLAST$^+$ stem cells to differentiating NBs. Under this condition, the expression of Nkx2.1 and Pbx3a in the lSVZ and vSVZ was indistinguishable between *Gsx2 GOF* mice and control mice (Supplemental Fig. 4J–K′). Thus, we did not find any indication that ectopic Gsx2 alters the regional identity of stem cells outside its normal expression domain. We found, however, that much smaller fractions of GFP$^+$ cells express Ki67, Ascl1, and Dlx2 in *Gsx2 GOF* mice (Fig. 5D). Instead, GFAP$^+$/EGFR$^+$ aNSCs

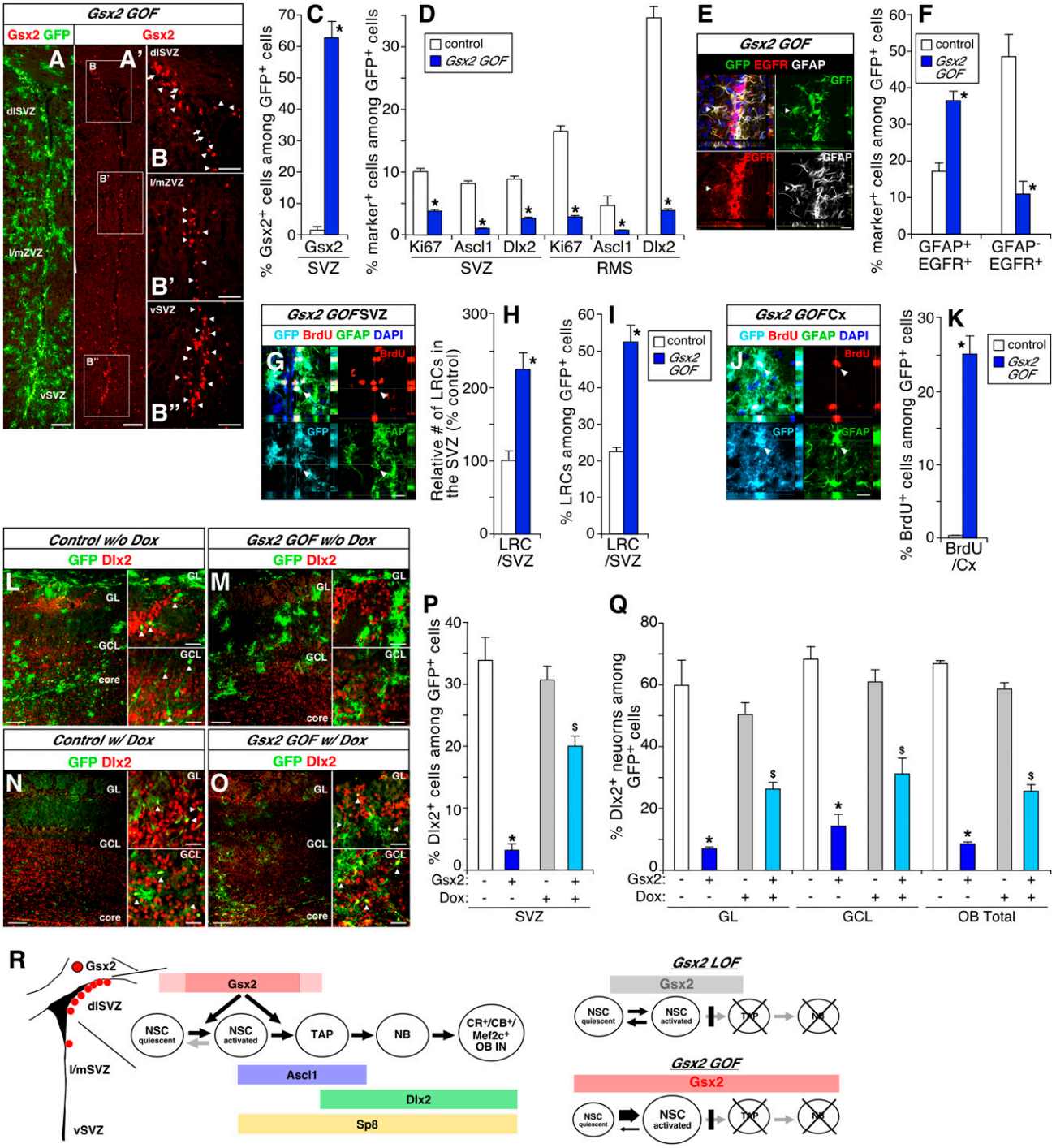

Figure 5. Gsx2 overexpression promotes transition from qNSCs to aNSCs. (*A–C*) Ectopic expression of Gsx2 in the SVZ of *Gsx2 GOF* mice at D56. Arrows and arrowheads indicate endogenous and ectopic Gsx2$^+$ cells, respectively. (*C*) Percentage of Gsx2$^+$ cells among GFP$^+$ cells in *Gsx2 GOF* and control mice at D56. (*D–I*) TAPs and NBs decrease and aNSCs accumulate in *Gsx2 GOF* mice. (*E,G*) Representative images of a GFP-labeled GFAP$^+$/EGFR$^+$ aNSC (arrowheads; *E*) and a BrdU-LRC (*G*) in *Gsx2 GOF* mice. (*F*) Percentages of GFAP$^+$/EGFR$^+$ aNSCs and GFAP$^-$/EGFR$^+$ TAPs among GFP$^+$ cells at D56. (*H,I*) Relative number of LRCs (*H*) and their percentage among GFP$^+$ cells (*I*) in the SVZ. BrdU was administered for 3 wk following overexpression of Gsx2 for 4 wk and was subsequently chased for additional 4 wk. (*J,K*) Gsx2 promotes proliferation of neocortical astrocytes. (*J*) Representative image of a BrdU$^+$/GFP$^+$ cortical astrocyte in *Gsx2 GOF* mice. (*K*) Percentage of BrdU$^+$ cells among GFP$^+$ cells in the neocortex (Cx). BrdU labeling was performed as described in *H* and *I*. (*L–O*) Inhibition of neurogenesis and its Dox-dependent restoration in *Gsx2 GOF* mice. GFP$^+$/Dlx2$^+$ OB neurons are detected in control mice under both Dox-untreated (*L*) and Dox-treated (*N*) conditions at D91, whereas such cells are much fewer in untreated *Gsx2 GOF* mice (*M*) and are partially restored by Dox treatment (*O*). (*P,Q*) The percentage of Dlx2$^+$ cells among GFP$^+$ cells in the SVZ (*P*) and GL, GCL, and total OB (*Q*) of Dox-treated and untreated animals. (*R*) A model for the action of Gsx2 in lineage progression of NSCs (*left*) and a summary of the phenotypes of *Gsx2* cKO and *GOF* mice (*right*). Vertical lines and thick arrows indicate blockage and promotion, respectively. Data are expressed as mean ± SEM of three animals. $P < 0.05$ compared with control (*) or Dox-untreated ($) animals. Bars: *A,A′,L–O*, 100 μm; *B,B′,E*, *insets* in *L–O*, 20 μm; *G,J*, 10 μm.

markedly increased at the expense of GFAP$^-$/EGFR$^+$ TAPs (Fig. 5E,F). Moreover, long-term BrdU labeling experiments detected more LRCs, and such BrdU$^+$ cells were highly enriched among GFP$^+$ cells (Fig. 5G–I). These results support the idea that the NSC pool expands at the expense of TAPs and NBs in *Gsx2 GOF* mice. As described above, although stem cell differentiation is blocked at the same step in *Gsx2* cKO mice, such blockage does not result in an increase of LRCs, suggesting that the failure of the transition from aNSCs to TAPs does not solely account for such an increase. Thus, it appears that in addition to being required for neurogenic progression, Gsx2 also promotes the transition from qNSCs to aNSCs and expands the stem cell pool. To further test this notion, we took advantage of the fact that our GOF approach drives ectopic expression of Gsx2 in astrocytes outside the neurogenic niche (Mori et al. 2006). Astrocytes in the neocortical gray matter and elsewhere in the brain rarely undergo cell divisions under normal conditions, although they share many features with SVZ stem cells (Pastrana et al. 2009; Beckervordersandforth et al. 2010). In fact, in control mice, few GFP$^+$ neocortical astrocytes incorporated BrdU under the condition in which LRCs were detected in the SVZ (Supplemental Fig. 4M). In contrast, >20% of GFP-labeled astrocytes were labeled with BrdU in *Gsx2 GOF* mice, demonstrating that Gsx2 induces otherwise quiescent cells to be proliferative (Fig. 5J,K; Supplemental Fig. 4N). These results support the idea that when overexpressed, Gsx2 promotes the transition from qNSCs to aNSCs, a critical first step in mobilization of NSCs.

Nevertheless, the aforementioned data show that a high level of Gsx2 blocks further lineage progression to TAPs. To further substantiate this idea, we examined the consequence of down-regulation of Gsx2 following overexpression. *Gsx2 GOF* and control mice were first treated with Tx and, 4 wk later, received Dox for 5 wk, during which new neurons generated by GFP$^+$ stem cells were allowed to migrate and settle in the OB. As expected, much weaker expression of GFP and Gsx2 was detected throughout the SVZ of these Dox-treated animals (Supplemental Fig. 4F–I′). However, we found that a much higher percentage of GFP$^+$ cells expresses Dlx2 in both the SVZ and the OB in Dox-treated *GOF* mice compared with untreated animals (Fig. 5N–Q). We also detected a higher percentage of GFP$^+$ cells coexpressing Ascl1, Ki67, and Dlx2 in the SVZ and RMS of Dox-treated mice, demonstrating Dox-dependent recovery of neurogenesis (Fig. 5P; Supplemental Fig. 4L). These results demonstrate that Gsx2 needs to be properly down-regulated for the progression from aNSCs to TAPs (summarized in Fig. 5R)

Role of Gsx2 in stem cell–niche interactions

Recent studies have uncovered the unique cytoarchitecture of the SVZ stem cell niche, in which NSCs maintain close contacts with both the ependymal layer (EPL) on the apical side and a vascular network embedded in the underlying SVZ on the basal side (Fuentealba et al. 2012). To reveal the role of Gsx2 in such niche–stem cell interactions, we obtained whole-mount preparations of the lateral wall of the LV from *Gsx2 GOF* and control mice and examined the behavior of GFP-labeled stem cell lineage cells in en face views of the niche (Fig. 6A). In control animals, the vast majority of GFP$^+$/Ki67$^+$ dividing cells formed tightly packed clusters around the SVZ vasculature, as described previously (Fig. 6B–B″; Shen et al. 2008; Tavazoie et al. 2008). In contrast, such cells were scarce and more scattered in *Gsx2 GOF* mice (Fig. 6C–C″). Moreover, the soma of GFP$^+$/Ki67$^+$ cells in *Gsx2 GOF* mice were often distant from the vascular network yet maintained contacts with nearby blood vessels by extending long processes (Fig. 6C–D′; Supplemental Movies S1, S2). These cells were reminiscent of ventricle-contacting apical stem cells described in previous studies (Mirzadeh et al. 2008; Kokovay et al. 2012).

We next examined the exact location of individual GFP$^+$/Ki67$^+$ cells along the apicobasal axis of the niche in a series of high-power z-stack images. Staining of adherens junctions with β-catenin (β-cat) antibody reveals the surface of the EPL and its honeycomb-like epithelial organization (Fig. 6E–F″; Supplemental Fig. 5). High-power views further show that the soma and short processes of apical GFP$^+$ cells are intercalated between ependymal cells (Fig. 6G–H′, arrowheads and asterisks) and express GFAP (Fig. 6I,I′). In control mice, these apically located cells represented about one-third (32.8%) of total GFP$^+$ cells, whereas the majority of them were located in the more basal SVZ region (Figure 6G′,K, arrows). Moreover, only a small fraction of these apical cells were Ki67$^+$, reflecting infrequent cell divisions of stem cells (Fig. 6G,J). In contrast, as much as 80% of GFP$^+$ cells were apically located in *Gsx2* cKO mice, and about one-half of these apical cells were costained for Ki67$^+$ (Fig. 6H′,J,K). Given the aforementioned results that Gsx2-overexpressing cells stall at the stage of aNSCs, these apically located dividing cells are likely to correspond to aNSCs, and the blockage of their lineage progression to TAPs correlates with the inhibition of downward translocation of their soma from the EPL to the SVZ along the apicobasal axis.

Gsx2 controls injury-induced neurogenesis

Previous studies have shown that various insults augment production of new neurons in the adult SVZ (Nakafuku and Grande 2013). The mechanisms underlying such injury-induced responses, however, remain largely unknown. We used two injury paradigms to ask whether Gsx2 plays any role in injury-induced neurogenesis. First, we used H/I injury, which causes broad hemilateral neocortical and striatal damage (Fig. 7A; Adhami et al. 2006). Surprisingly, H/I not only increased the number of Gsx2$^+$ cells in its normal expression domain, but also induced ectopic Gsx2$^+$ cells in the lateral and ventral regions of the SVZ 7 d after injury (Fig. 7B–D′). A significant increase in Gsx2$^+$ cells was apparent even in the contralateral hemisphere compared with uninjured animals, but much stronger induction was detected in the ipsilateral SVZ (Fig. 7D). Accompa-

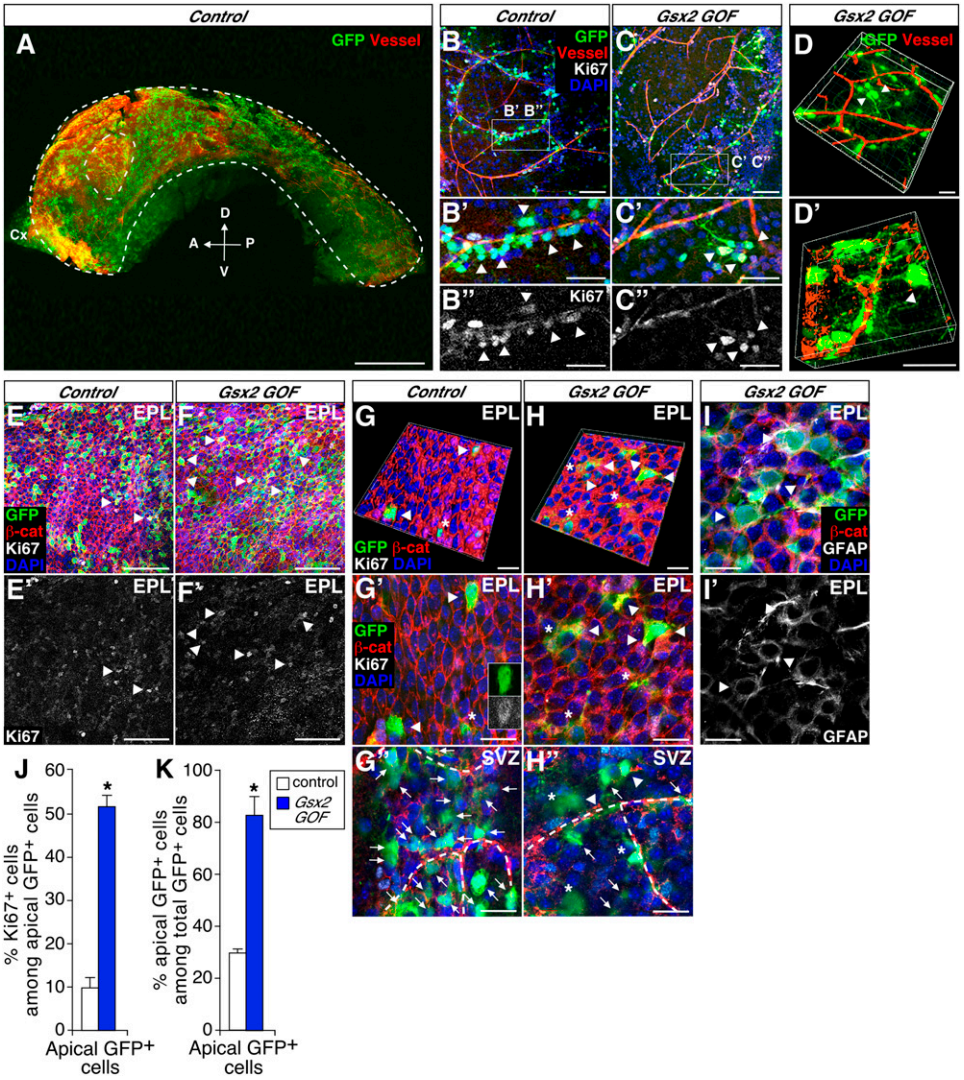

Figure 6. Gsx2 promotes proliferation of apical stem cells. (*A*) A whole-mount preparation of the lateral wall of the LV from *Gsx2 GOF* mice. GFP$^+$ recombined cells (green), blood vessels (red), and DAPI$^+$ nuclei (blue) are visualized. (*B–D*) Association of GFP$^+$/Ki67$^+$ cells with the SVZ vasculature in control (*B–B″*) and *Gsx2 GOF* (*C–C″*) mice. (*D*,*D′*) Representative three-dimensional (3D) reconstruction images of GFP$^+$/Ki67$^+$ cells that maintain contact with nearby blood vessels (red) with long processes in *Gsx2 GOF* mice. Rotating 3D images are available as Supplemental Movies S1 and S2. (*E–F′*) GFP$^+$/Ki67$^+$ proliferative apical cells (arrowheads) in control (*E*,*E′*) and *Gsx2 GOF* (*F*,*F′*) mice. (*G–H″*) Confocal images of the soma (arrowheads) and processes (asterisks) of a GFP$^+$/Ki67$^+$ cell at the apical surface of the EPL (*G*,*G′*,*H*,*H′*) and the SVZ (arrowheads and *insert* in *G″*,*H″*). (*G*,*H*) 3D reconstruction images of the EPL. (*G′*,*H′*) En face views of the same areas shown in *G* and *H*. Dashed lines in *G″* and *H′* indicate blood vessels running through the SVZ. Note that many GFP signals detected at the SVZ level in *H″* (arrowheads) are the soma of apically located GFP$^+$ cells shown in *H*. (*I*,*I′*) GFP$^+$/GFAP$^+$ apical cells (arrowheads) in *Gsx2 GOF* mice. (*J*,*K*) The percentage of Ki67$^+$ dividing cells among apically located GFP$^+$ cells (*J*) and apical GFP$^+$ cells among total GFP$^+$ cells (*K*). Data are expressed as mean ± SEM of three animals. (*) $P < 0.05$ compared with control animals. Bars: *A*, 1000 μm, *B*,*C*,*E–F′*, 100 μm; *B″–C″*, 50 μm; *D*,*D′*, 20 μm.

nying this Gsx2 up-regulation, Ki67$^+$ proliferative cells, Ascl1$^+$ TAPs, and Dlx2$^+$ NBs all increased in broad SVZ regions after H/I (Fig. 7E–G).

Similar induction of Gsx2 was observed following more localized brain injury. Stereotaxic injection of a small amount of the glutamate receptor agonist quinolinic acid (QA) into the striatum causes focal excitotoxic neuronal loss (Fig. 7H; Hansson et al. 1999). We compared the expression of Gsx2 and the level of neurogenesis between ipsilateral and contralateral SVZs after hemilateral QA injury. To reveal the role of Gsx2 in injury responses, we performed the same analyses using *Gsx2* cKO and control mice. Like in the H/I model, we detected a significant increase of Gsx2$^+$ cells in the ipsilateral SVZ compared with the contralateral side, and such an increase occurred not only in the dlSVZ, but also in the lateral and ventral regions (Fig. 7I). This ectopic induction of Gsx2 accompanied increased production of new neurons in the SVZ as revealed by the up-regulation of Ki67$^+$, Ascl1$^+$, and Dlx2$^+$ cells in control animals (Fig. 7J). Moreover, ectopic Sp8$^+$

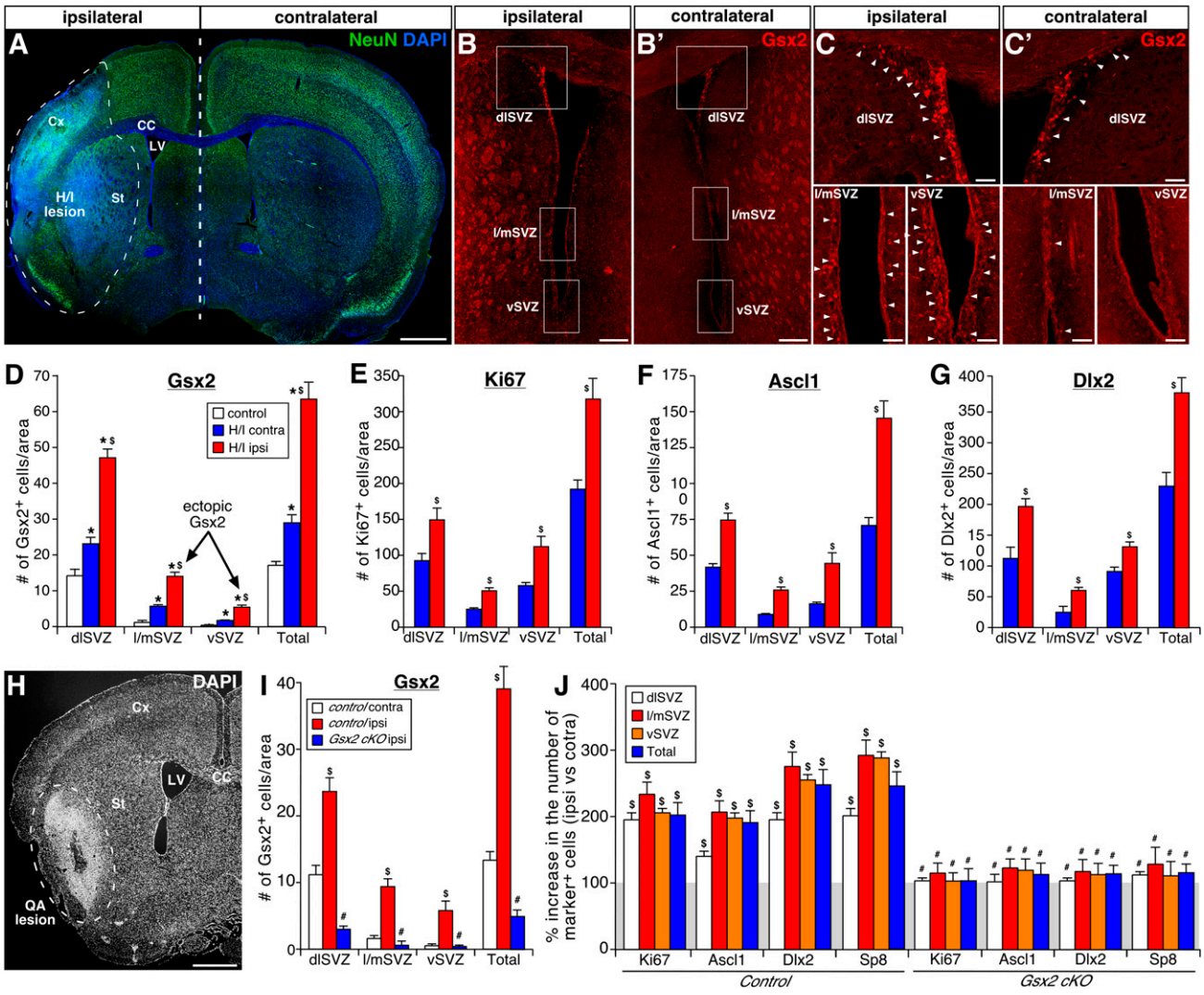

Figure 7. Ectopic induction of Gsx2 is required for injury-induced neurogenesis. (*A*) A NeuN/DAPI-stained coronal section of a H/I brain showing widespread damage in the neocortex and striatum (dashed circle) 7 d after H/I. (*B–D*) Enhanced and ectopic expression of Gsx2 after H/I. Images show Gsx2$^+$ cells (arrowheads) in the ipsilateral (*B*,*C*) and contralateral (*B′*,*C′*) hemispheres. (*D–G*) Quantitative analysis of Gsx2$^+$ (*D*), Ki67$^+$ (*E*), Ascl1$^+$ (*F*), and Dlx2$^+$ (*G*) cells in SVZ subregions of the ipsilateral (ipsi) and contralateral (contra) hemispheres 7 d after H/I compared with uninjured control animals. (*H*) A DAPI-stained QA-injured brain showing focal damage in the striatum (dashed circle) 7 d after QA injury. (*I*) Enhanced and ectopic expression of Gsx2 after QA injury in control animals and the lack thereof in *Gsx2* cKO mice. (*J*) The percentage increases of Ki67$^+$, Ascl1$^+$, Dlx2$^+$, and Sp8$^+$ cells in the ipsilateral SVZ relative to the contralateral side in control (*left*) and *Gsx2* cKO (*right*) mice. Data in graphs are expressed as mean ± SEM of four animals for each genotype. $P < 0.05$ compared with uninjured animals (* in *D*), the contralateral hemisphere ($ in *D–G*,*I*,*J*), or control animals (# in *I*,*J*). Bars: *A*,*H*, 1000 μm; *B*,*B′*, 200 μm; *C*,*C′*, 20 μm.

cells, which are normally produced by Gsx2$^+$ NSCs in the dlSVZ, were detected in the lSVZ and vSVZ (Fig. 7J). Importantly, such injury-induced responses were almost completely abolished in *Gsx2* cKO mice (Fig. 7J). It is particularly noteworthy that the up-regulation of neurogenesis was halted not only in the normal Gsx2-expressing region (dlSVZ), but also in its ectopic expression sites (lSVZ and vSVZ). This is surprising given the fact that inactivation of Gsx2 does not affect the baseline neurogenesis in these regions in the intact brain. These results demonstrate that Gsx2 is not only required for continuous neurogenesis in a specific subregion of the SVZ in the intact brain, but is also essential for injury-induced neurogenesis in broader SVZ regions after insult.

Discussion

Regional heterogeneity of adult NSCs

Recent studies have demonstrated that adult NSCs are regionally heterogeneous (Lledo et al. 2008 and references therein). Details of such heterogeneity, however, remain poorly understood. This study provides new insights into this issue and highlights similarities and differences

between embryonic and adult NSCs. During embryogenesis, Gsx2 expression becomes refined to a high dorsal–low ventral gradient within the lateral ganglionic eminence (LGE) at late embryonic stages. The high-Gsx-expressing region defines the dLGE that serves as a major source of embryonically generated OB interneurons (Yun et al. 2001; Stenman et al. 2003; Waclaw et al. 2009). Similarly, the adult expression of Gsx2 is mostly confined to the dlSVZ and plays an essential role in proper OB neurogenesis in this region. These similarities support the idea that the embryonic dLGE is the origin of the dlSVZ in adults. In fact, a previous lineage tracing study has shown that this adult region contains progeny of embryonic Gsx2$^+$ progenitors (Young et al. 2007). Moreover, the adult Gsx2$^+$ domain is flanked by Pax6$^+$ cells dorsally and Gsx1$^+$ and Nkx2.1$^+$ cells ventrally, and a similar topological organization of germinal zones has been reported in the developing telencephalon (Stenman et al. 2003; Waclaw et al. 2006, 2009), supporting the idea that the DV organization of progenitor domains is preserved between embryos and adults.

Nevertheless, this study has also revealed a clear difference between embryonic and adult NSCs. During development, the positional identity of progenitors is established through cross-suppression between region-specific factors, and therefore, inactivation of one of these factors often results in the expansion of adjacent domains (Puelles and Rubenstein 2003). For instance, in the telencephalon of *Gsx2* KO embryos, the Pax6$^+$ dorsal domain expands ventrally, and the Gsx1$^+$ ventral domain invades dorsally into the normally Gsx2$^+$ domain (Toresson et al. 2000; Toresson and Campbell 2001; Yun et al. 2001, 2003). However, we did not find evidence for such misspecification in adult *Gsx2* cKO or *GOF* mice. It could be that once the regional specificity is established during embryogenesis, the identities of distinct NSC groups are maintained independently from each other at the adult stage. Alternatively, the local environment plays a predominant role in maintaining the stem cell identity. In fact, a recent study has proposed that Shh signals play a role in specifying NSCs in the vSVZ (Ihrie et al. 2011). Our data using *Gli1-nLacZ* mice, however, suggest that Gsx2 is not under the direct influence of Shh signals in the dlSVZ and that ectopic Gsx2 does not override the specificity of vSVZ stem cells.

NSCs and OB interneuron diversity

Adult inactivation of Gsx2 selectively attenuates the production of CR$^+$, NC$^+$, and CB$^+$ interneurons in the GL and Mef2c$^+$ cells in the GCL of the OB. In parallel, we detected a marked reduction of Sp8$^+$ cells in the SVZ, RMS, and OB, which is essential for proper differentiation of CR$^+$ GL neurons in embryos (Waclaw et al. 2006). Thus, Sp8 appears to be a crucial downstream target of Gsx2 in producing CR$^+$ GL neurons in the adult brain. Whether the reduced Sp8$^+$ cell number also accounts for the reduction of other adult-born neuronal subtypes in the cKO mice remains to be determined. Pax6, which is required for differentiation of TH$^+$ neurons in the GL and granule cells in the superficial GCL (Hack et al. 2005; Kohwi et al. 2005), is also attenuated in the dlSVZ but not in the RMS or OB, and we detected no apparent change in the production of these neuronal subtypes in *Gsx2* cKO mice.

Previous studies have provided a link between the anatomical location of NSCs and the subtype specificity of their neuronal progeny in the early postnatal brain (Lledo et al. 2008). Given the regionally restricted expression of Gsx2, the above results suggest that Gsx2$^+$ NSCs in the dlSVZ and RMS are the major source of the neuronal subtypes lost in the cKO mice. However, we detected an incomplete loss of these neuronal subtypes in the mutant. A likely explanation for this is that inactivation of Gsx2 was incomplete, in particular, in the RMS in the mutant. Another possibility is that non-Gsx2$^+$ NSCs in other regions also contribute to their production. In fact, the correlation between the location of NSCs and the subtype specificity of their progeny appears not to be strict; NSCs located at a particular region generate more than one neuronal subtype, and those in different regions produce overlapping subtypes (Merkle et al. 2007). Perhaps molecular markers currently available do not fully distinguish all OB neuronal subtypes, and Gsx2$^+$ NSC-derived neurons represent only a specific subset. Alternatively, NSCs residing in a given SVZ region could be heterogeneous, and Gsx2$^+$ NSCs coexist with other stem cell subtypes in the same region.

Mobilization and lineage progression of adult NSCs

Many molecules act as common regulators of stem/progenitor cells in embryos and adults (Ninkovic and Götz 2007). However, the long-term maintenance of quiescent and slowly cycling stem cells and their progression to actively proliferating TAPs are unique to adult NSCs. Our data have demonstrated that Gsx2 plays a crucial role in these adult-specific regulatory steps. Gsx2 is expressed in aNSCs and TAPs and is subsequently down-regulated, while cells further progress toward NBs. Both inactivation and constitutive overexpression of Gsx2 block the transition from aNSCs to TAPs, suggesting that the temporally controlled induction and down-regulation of Gsx2 is important for proper lineage progression of adult NSCs. In this regard, Gsx2 can be considered as a gatekeeper that controls the tempo of adult neurogenesis. We also found that overexpression of Gsx2 promotes the mobilization of qNSCs toward aNSCs and expands the stem cell pool. However, we did not detect a significant reduction of NSCs in *Gsx2* cKO mice, suggesting that other molecules also play a redundant role in regulating this step.

Recent studies have revealed that the maintenance and activity of adult NSCs is tightly controlled by signals from their niche (Fuentealba et al. 2012; Song et al. 2012). However, cell-intrinsic regulators that operate downstream from such niche signals are not well understood. Our data suggest that Gsx2 acts as such a cell-intrinsic regulator in a subset of stem cells. In *Gsx2 GOF* mice, aNSCs accumulate in the EPL, the apical niche, yet actively divide at locations away from the basal vascular

niche. Such cell divisions distant from the vasculature, however, are much less frequent in control animals. Thus, we speculate that one of the roles of vascular niche signals is to turn on Gsx2 or its equivalents in quiescent stem cells and initiate their mobilization.

Importantly, Gsx2 exerts such a function only in a restricted subset of NSCs. Thus, this study has uncovered a previously unrecognized mode of regulation of adult NSCs; distinct molecules mobilize stem cells toward neurogenesis in different regions. We speculate that other molecules play a similar role in other NSC populations and that Gsx1, a close homolog of Gsx2, is a likely candidate in the lSVZ and vSVZ. Interestingly, downstream from these region-specific regulators, some common mechanisms operate across stem cell niches. The bHLH factor Ascl1 and the homeodomain factor Dlx2 are commonly expressed in TAPs and NBs, respectively, throughout SVZ subregions and play important roles in the production of new neurons (Brill et al. 2008; Kim et al. 2011; A López-Juárez and M Nakafuku, unpubl.). Our data place Gsx2 as an upstream regulator of these factors selectively in the dlSVZ. This two-step regulatory mechanism could explain, at least in part, how distinct adult NSC pools as a whole generate a diverse array of OB neurons that share many common features yet exhibit distinct phenotypes.

Mechanisms for injury-induced neurogenesis

A variety of insults, including ischemia, trauma, excitotoxicity, and neurodegeneration, stimulate neurogenesis in the adult brain (Nakafuku and Grande 2013). The mechanisms underlying such injury-induced neurogenesis, however, remain largely unknown. We identified Gsx2 as a crucial regulator of such regenerative responses. In particular, our studies have revealed two previously unrecognized features of neurogenesis after injury. First, both H/I and QA injury up-regulate Gsx2 not only in its normal expression domain, but also in much broader SVZ subregions. Thus, injury does not simply raise the level of activity of endogenous NSCs but rather modulates their molecular features in a unique way. Second, inactivation of Gsx2 abrogates injury-induced neurogenesis throughout the SVZ, indicating that ectopically expressed Gsx2 is essential for injury-induced responses even in regions that do not normally depend on Gsx2. It remains unknown why other molecules that control continuous neurogenesis in these normally Gsx2-negative domains are insufficient for injury responses. These unexpected findings have revealed that distinct mechanisms control neurogenesis in intact and injured brains. A recent study using zebrafish has shown that injury-induced GATA3 plays a crucial role in regenerating neurons lost to insult (Kizil et al. 2012). A similarity between GATA3 in zebrafish and Gsx2 in mice is that both are broadly up-regulated by injury and are essential for stimulation of neurogenesis. An important difference, however, is that Gsx2 is expressed in a subset of stem cells in the intact brain, whereas GATA3 expression appears to be specific to injured brains.

Our finding also provides new insights into the plasticity of adult NSCs. The fact that injury induces ectopic expression of Gsx2 in normally nonexpressing regions raises the possibility that injury alters the regional specificity of NSCs. This idea is particularly intriguing in light of the previous finding that in response to various insults, the adult SVZ not only generates more OB neurons, but also produces new neurons that migrate toward lesion sites outside the normal neurogenic niches, and these new neurons exhibit region-appropriate phenotypes (Nakafuku and Grande 2013). If NSCs normally committed to the generation of OB neurons are responsible for the production of such non-OB neurons after injury, it likely occurs through respecification of their identity, and ectopic expression of Gsx2 in response to injury could be part of such respecification. Alternatively, injury-induced Gsx2 may mobilize NSCs that otherwise remain dormant and do not participate in OB neurogenesis in the intact brain to produce new neurons in damaged regions. Further studies on the role of Gsx2 in damaged brains will contribute to future development of strategies to augment endogenous regenerative capacities toward better recovery and repair after injury.

Materials and methods

Animals

All procedures were performed using young adult animals at the age of 8–12 wk according to the guidelines of the National Institutes of Health and the Institutional Animal Care and Use Committee. Details of the source of animals and the breeding and handling procedures are described in the Supplemental Material.

Injury models

Unilateral H/I injury was performed as described previously (Adhami et al. 2006). Procedures for focal striatal injury with QA followed a method described previously (Hansson et al. 1999). Details are described in the Supplemental Material.

Histology

For immunostaining, 12-μm-thick cryosections or 25-μm-thick vibratome sections of 4% (v/v) paraformaldehyde-fixed brains were used. Whole-mounts of the lateral wall of the LV were prepared as described previously (Mirzadeh et al. 2010). The method to identify specific regions of the neurogenic niche and antibodies used for immunostaining is described in the Supplemental Material. Immunoreactive cells were visualized by staining with secondary antibodies conjugated with Alexa Fluor 488, 568, and 647 (Invitrogen). Fluorescent images were captured by a CCD camera attached to Carl Zeiss Axiophoto II or Apotome. Z-stack images of whole mounts were obtained using Nikon A1R si laser-scanning confocal microscope. The quantitative results are expressed as mean ± standard error of the mean (SEM) of data obtained from three to four mice, and statistical analyses were performed with two-tailed unpaired *t*-test.

Acknowledgments

We are grateful to Magdalena Götz, Jane Johnson, Martyn Goulding, and Kazuaki Yoshikawa for reagents; Matthew Kofron

for technical support for imaging; and Anna Nelke, Felicia Rinaldi, Rohit Rao, and Christine Marques for participation in an initial phase of the project. This study is supported by NIH/NINDS 1R01NS069893 to M.N. and K.C., NIH/NINDS R01NS044080 to K.C., Ohio Eminent Scholar Fund from the State of Ohio to M.N., and CONACyT162786 to A.L.J.

References

Adhami F, Liao G, Morozov YM, Schloemer A, Schmithorst VJ, Lorenz JN, Dunn RS, Vorhees CV, Wills-Karp M, Degen JL, et al. 2006. Cerebral ischemia–hypoxia induces intravascular coagulation and autophagy. *Am J Pathol* **169:** 566–583.

Bai CB, Auerbach W, Lee JS, Stephen D, Joyner AL. 2002. Gli2, but not Gli1, is required for initial Shh signaling and ectopic activation of the Shh pathway. *Development* **129:** 4753–4761.

Balordi F, Fishell G. 2007. Mosaic removal of hedgehog signaling in the adult SVZ reveals that the residual wild-type stem cells have a limited capacity for self-renewal. *J Neurosci* **27:** 14248–14259.

Basak O, Giachino C, Fiorini E, Macdonald HR, Taylor V. 2012. Neurogenic subventricular zone stem/progenitor cells are Notch1-dependent in their active but not quiescent state. *J Neurosci* **32:** 5654–5666.

Beckervordersandforth R, Tripathi P, Ninkovic J, Bayam E, Lepier A, Stempfhuber B, Kirchhoff F, Hirrlinger J, Haslinger A, Lie DC, et al. 2010. In vivo fate mapping and expression analysis reveals molecular hallmarks of prospectively isolated adult neural stem cells. *Cell Stem Cell* **7:** 744–758.

Bonaguidi MA, Wheeler MA, Shapiro JS, Stadel RP, Sun GJ, Ming GL, Song H. 2011. In vivo clonal analysis reveals self-renewing and multipotent adult neural stem cell characteristics. *Cell* **145:** 1142–1155.

Brill MS, Snapyan M, Wohlfrom H, Ninkovic J, Jawerka M, Mastick GS, Ashery-Padan R, Saghatelyan A, Berninger B, Götz M. 2008. A dlx2- and pax6-dependent transcriptional code for periglomerular neuron specification in the adult olfactory bulb. *J Neurosci* **28:** 6439–6452.

Brill MS, Ninkovic J, Winpenny E, Hodge RD, Ozen I, Yang R, Lepier A, Gascon S, Erdelyi F, Szabo G, et al. 2009. Adult generation of glutamatergic olfactory bulb interneurons. *Nat Neurosci* **12:** 1524–1533.

Briñón JG, Martinez-Guijarro FJ, Bravo IG, Arevalo R, Crespo C, Okazaki K, Hidaka H, Aijon J, Alonso JR. 1999. Coexpression of neurocalcin with other calcium-binding proteins in the rat main olfactory bulb. *J Comp Neurol* **407:** 404–414.

Doetsch F, Caille I, Lim DA, Garcia-Verdugo JM, Alvarez-Buylla A. 1999. Subventricular zone astrocytes are neural stem cells in the adult mammalian brain. *Cell* **97:** 703–716.

Fuentealba LC, Obernier K, Alvarez-Buylla A. 2012. Adult neural stem cells bridge their niche. *Cell Stem Cell* **10:** 698–708.

Giachino C, Taylor V. 2009. Lineage analysis of quiescent regenerative stem cells in the adult brain by genetic labelling reveals spatially restricted neurogenic niches in the olfactory bulb. *Eur J Neurosci* **30:** 9–24.

Gong S, Zheng C, Doughty ML, Losos K, Didkovsky N, Schambra UB, Nowak NJ, Joyner A, Leblanc G, Hatten ME, et al. 2003. A gene expression atlas of the central nervous system based on bacterial artificial chromosomes. *Nature* **425:** 917–925.

Gritti A, Bonfanti L, Doetsch F, Caille I, Alvarez-Buylla A, Lim DA, Galli R, Verdugo JM, Herrera DG, Vescovi AL. 2002. Multipotent neural stem cells reside into the rostral extension and olfactory bulb of adult rodents. *J Neurosci* **22:** 437–445.

Hack MA, Saghatelyan A, de Chevigny A, Pfeifer A, Ashery-Padan R, Lledo PM, Götz M. 2005. Neuronal fate determinants of adult olfactory bulb neurogenesis. *Nat Neurosci* **8:** 865–872.

Hansson O, Petersen A, Leist M, Nicotera P, Castilho RF, Brundin P. 1999. Transgenic mice expressing a Huntington's disease mutation are resistant to quinolinic acid-induced striatal excitotoxicity. *Proc Natl Acad Sci* **96:** 8727–8732.

Ihrie RA, Shah JK, Harwell CC, Levine JH, Guinto CD, Lezameta M, Kriegstein AR, Alvarez-Buylla A. 2011. Persistent sonic hedgehog signaling in adult brain determines neural stem cell positional identity. *Neuron* **71:** 250–262.

Kaslin J, Ganz J, Brand M. 2008. Proliferation, neurogenesis and regeneration in the non-mammalian vertebrate brain. *Philos Trans R Soc Lond B Biol Sci* **363:** 101–122.

Kim EJ, Ables JL, Dickel LK, Eisch AJ, Johnson JE. 2011. Ascl1 (Mash1) defines cells with long-term neurogenic potential in subgranular and subventricular zones in adult mouse brain. *PLoS ONE* **6:** e18472.

Kizil C, Kyritsis N, Dudczig S, Kroehne V, Freudenreich D, Kaslin J, Brand M. 2012. Regenerative neurogenesis from neural progenitor cells requires injury-induced expression of gata3. *Dev Cell* **23:** 1230–1237.

Kohwi M, Osumi N, Rubenstein JL, Alvarez-Buylla A. 2005. Pax6 is required for making specific subpopulations of granule and periglomerular neurons in the olfactory bulb. *J Neurosci* **25:** 6997–7003.

Kokovay E, Wang Y, Kusek G, Wurster R, Lederman P, Lowry N, Shen Q, Temple S. 2012. VCAM1 is essential to maintain the structure of the SVZ niche and acts as an environmental sensor to regulate SVZ lineage progression. *Cell Stem Cell* **11:** 220–230.

Kriks S, Lanuza GM, Mizuguchi R, Nakafuku M, Goulding M. 2005. Gsh2 is required for the repression of Ngn1 and specification of dorsal interneuron fate in the spinal cord. *Development* **132:** 2991–3002.

Lemasson M, Saghatelyan A, Olivo-Marin JC, Lledo PM. 2005. Neonatal and adult neurogenesis provide two distinct populations of newborn neurons to the mouse olfactory bulb. *J Neurosci* **25:** 6816–6825.

Lledo PM, Merkle FT, Alvarez-Buylla A. 2008. Origin and function of olfactory bulb interneuron diversity. *Trends Neurosci* **31:** 392–400.

Lyons GE, Micales BK, Schwarz J, Martin JF, Olson EN. 1995. Expression of mef2 genes in the mouse central nervous system suggests a role in neuronal maturation. *J Neurosci* **15:** 5727–5738.

Maslov AY, Barone TA, Plunkett RJ, Pruitt SC. 2004. Neural stem cell detection, characterization, and age-related changes in the subventricular zone of mice. *J Neurosci* **24:** 1726–1733.

Merkle FT, Mirzadeh Z, Alvarez-Buylla A. 2007. Mosaic organization of neural stem cells in the adult brain. *Science* **317:** 381–384.

Ming GL, Song H. 2005. Adult neurogenesis in the mammalian central nervous system. *Annu Rev Neurosci* **28:** 223–250.

Mirzadeh Z, Merkle FT, Soriano-Navarro M, Garcia-Verdugo JM, Alvarez-Buylla A. 2008. Neural stem cells confer unique pinwheel architecture to the ventricular surface in neurogenic regions of the adult brain. *Cell Stem Cell* **3:** 265–278.

Mirzadeh Z, Doetsch F, Sawamoto K, Wichterle H, Alvarez-Buylla A. 2010. The subventricular zone en-face: Wholemount staining and ependymal flow. *J Vis Exp* **39:** e1938.

Mori T, Tanaka K, Buffo A, Wurst W, Kuhn R, Götz M. 2006. Inducible gene deletion in astroglia and radial glia—a valuable tool for functional and lineage analysis. *Glia* **54:** 21–34.

Morshead CM, Reynolds BA, Craig CG, McBurney MW, Staines WA, Morassutti D, Weiss S, van der Kooy D. 1994. Neural stem cells in the adult mammalian forebrain: A relatively quiescent subpopulation of subependymal cells. *Neuron* **13:** 1071–1082.

Nakafuku M, Grande A. 2013. Neurogenesis in the damaged mammalian brain. In *Patterning and cell type specification in the developing CNS and PNS: comprehensive developmental neuroscience* (ed. Rubenstein JLR, Rakic P). Elsevier, Maryland Heights, MO (in press).

Nakamura T, Colbert MC, Robbins J. 2006. Neural crest cells retain multipotential characteristics in the developing valves and label the cardiac conduction system. *Circ Res* **98:** 1547–1554.

Nakatomi H, Kuriu T, Okabe S, Yamamoto S, Hatano O, Kawahara N, Tamura A, Kirino T, Nakafuku M. 2002. Regeneration of hippocampal pyramidal neurons after ischemic brain injury by recruitment of endogenous neural progenitors. *Cell* **110:** 429–441.

Ninkovic J, Götz M. 2007. Signaling in adult neurogenesis: From stem cell niche to neuronal networks. *Curr Opin Neurobiol* **17:** 338–344.

Parrish-Aungst S, Shipley MT, Erdelyi F, Szabo G, Puche AC. 2007. Quantitative analysis of neuronal diversity in the mouse olfactory bulb. *J Comp Neurol* **501:** 825–836.

Pastrana E, Cheng LC, Doetsch F. 2009. Simultaneous prospective purification of adult subventricular zone neural stem cells and their progeny. *Proc Natl Acad Sci* **106:** 6387–6392.

Pei Z, Wang B, Chen G, Nagao M, Nakafuku M, Campbell K. 2011. Homeobox genes Gsx1 and Gsx2 differentially regulate telencephalic progenitor maturation. *Proc Natl Acad Sci* **108:** 1675–1680.

Ponti G, Obernier K, Guinto C, Jose L, Bonfanti L, Alvarez-Buylla A. 2013. Cell cycle and lineage progression of neural progenitors in the ventricular-subventricular zones of adult mice. *Proc Natl Acad Sci* **110:** E1045–E1054.

Puelles L, Rubenstein JL. 2003. Forebrain gene expression domains and the evolving prosomeric model. *Trends Neurosci* **26:** 469–476.

Shen Q, Wang Y, Kokovay E, Lin G, Chuang SM, Goderie SK, Roysam B, Temple S. 2008. Adult SVZ stem cells lie in a vascular niche: A quantitative analysis of niche cell-cell interactions. *Cell Stem Cell* **3:** 289–300.

Shook BA, Manz DH, Peters JJ, Kang S, Conover JC. 2012. Spatiotemporal changes to the subventricular zone stem cell pool through aging. *J Neurosci* **32:** 6947–6956.

Simons BD, Clevers H. 2011. Strategies for homeostatic stem cell self-renewal in adult tissues. *Cell* **145:** 851–862.

Song J, Zhong C, Bonaguidi MA, Sun GJ, Hsu D, Gu Y, Meletis K, Huang ZJ, Ge S, Enikolopov G, et al. 2012. Neuronal circuitry mechanism regulating adult quiescent neural stem-cell fate decision. *Nature* **489:** 150–154.

Stenman J, Toresson H, Campbell K. 2003. Identification of two distinct progenitor populations in the lateral ganglionic eminence: Implications for striatal and olfactory bulb neurogenesis. *J Neurosci* **23:** 167–174.

Szucsik JC, Witte DP, Li H, Pixley SK, Small KM, Potter SS. 1997. Altered forebrain and hindbrain development in mice mutant for the Gsh-2 homeobox gene. *Dev Biol* **191:** 230–242.

Tavazoie M, Van der Veken L, Silva-Vargas V, Louissaint M, Colonna L, Zaidi B, Garcia-Verdugo JM, Doetsch F. 2008. A specialized vascular niche for adult neural stem cells. *Cell Stem Cell* **3:** 279–288.

Toresson H, Campbell K. 2001. A role for Gsh1 in the developing striatum and olfactory bulb of Gsh2 mutant mice. *Development* **128:** 4769–4780.

Toresson H, Potter SS, Campbell K. 2000. Genetic control of dorsal-ventral identity in the telencephalon: Opposing roles for Pax6 and Gsh2. *Development* **127:** 4361–4371.

Waclaw RR, Allen ZJ 2nd, Bell SM, Erdelyi F, Szabo G, Potter SS, Campbell K. 2006. The zinc finger transcription factor Sp8 regulates the generation and diversity of olfactory bulb interneurons. *Neuron* **49:** 503–516.

Waclaw RR, Wang B, Pei Z, Ehrman LA, Campbell K. 2009. Distinct temporal requirements for the homeobox gene Gsx2 in specifying striatal and olfactory bulb neuronal fates. *Neuron* **63:** 451–465.

Wang L, Sharma K, Deng HX, Siddique T, Grisotti G, Liu E, Roos RP. 2008. Restricted expression of mutant SOD1 in spinal motor neurons and interneurons induces motor neuron pathology. *Neurobiol Dis* **29:** 400–408.

Wang B, Waclaw RR, Allen ZJ 2nd, Guillemot F, Campbell K. 2009. Ascl1 is a required downstream effector of Gsx gene function in the embryonic mouse telencephalon. *Neural Dev* **4:** 5.

Young KM, Fogarty M, Kessaris N, Richardson WD. 2007. Subventricular zone stem cells are heterogeneous with respect to their embryonic origins and neurogenic fates in the adult olfactory bulb. *J Neurosci* **27:** 8286–8296.

Yun K, Potter S, Rubenstein JL. 2001. Gsh2 and Pax6 play complementary roles in dorsoventral patterning of the mammalian telencephalon. *Development* **128:** 193–205.

Yun K, Garel S, Fischman S, Rubenstein JL. 2003. Patterning of the lateral ganglionic eminence by the Gsh1 and Gsh2 homeobox genes regulates striatal and olfactory bulb histogenesis and the growth of axons through the basal ganglia. *J Comp Neurol* **461:** 151–165.

Zhao C, Deng W, Gage FH. 2008. Mechanisms and functional implications of adult neurogenesis. *Cell* **132:** 645–660.

Gsx2 controls region-specific activation of neural stem cells and injury-induced neurogenesis in the adult subventricular zone

Alejandro López-Juárez, Jennifer Howard, Kristy Ullom, et al.

Genes Dev. 2013, **27:** originally published online May 30, 2013
Access the most recent version at doi:10.1101/gad.217539.113